Developmental Cell, Vol. 1, 291–302, August, 2001, Copyright ©2001 by Cell Press

A Viral Phospholipase A_2 Is Required for Parvovirus Infectivity

Zoltán Zádori,[1] József Szelei,[1] Marie-Claude Lacoste,[1] Yi Li,[1] Sébastien Gariépy,[1] Philippe Raymond,[1] Marc Allaire,[1] Ivan R. Nabi,[2] and Peter Tijssen[1,3]

[1] Centre de microbiologie et biotechnologie
INRS-Institut Armand-Frappier
Université du Québec
531 boul. des Prairies
Laval, Québec H7V 1B7
Canada

[2] Département de pathologie et biologie cellulaire
Université de Montréal
Montréal, Québec H3T 1J4
Canada

Summary

Sequence analysis revealed phospholipase A_2 (PLA_2) motifs in capsid proteins of parvoviruses. Although PLA_2 activity is not known to exist in viruses, putative PLA_2s from divergent parvoviruses, human B19, porcine parvovirus, and insect *Gm*DNV (densovirus from *Galleria mellonella*), can emulate catalytic properties of secreted PLA_2. Mutations of critical amino acids strongly reduce both PLA_2 activity and, proportionally, viral infectivity, but cell surface attachment, entry, and endocytosis by PLA_2-deficient virions are not affected. PLA_2 activity is critical for efficient transfer of the viral genome from late endosomes/lysosomes to the nucleus to initiate replication. These findings offer the prospect of developing PLA_2 inhibitors as a new class of antiviral drugs against parvovirus infections and associated diseases.

Introduction

Parvoviruses infect vertebrates and invertebrates and occasionally emerge in new hosts. Newly arisen parvoviruses may cause pandemics with high mortality rates as demonstrated by the sudden appearance of canine parvovirus (CPV) during the late 1970s (Parrish, 1999). Parvoviruses depend on the S phase of the host cell for replication (Berns, 1996). This predilection for dividing cells is reflected in a wide tropism of the virus for fetal tissues compared to the narrower range of cells affected in adult animals. The human parvovirus B19 causes erythema infectiosum, a childhood disease, hydrops fetalis, and abortion (Brown, 2000). It has also been associated with different autoimmune diseases such as rheumatoid arthritis (RA), systemic lupus erythematosus (SLE), adult-onset Still's disease, and polyarthritis (Foto et al., 1993; Ytterberg, 1999). Virus-associated arthropathy is usually self-limiting and transient (Takahashi et al., 1998a). Findings that B19 initiates and perpetuates RA (Takahashi et al., 1998b) remain to be confirmed (Moore, 2000).

Parvoviruses package a single-stranded DNA into a nonenveloped, icosahedral capsid. Some passive roles have been attributed to the capsid, such as the protection of the viral genome, cell receptor recognition, and host specificity (Gardiner and Tattersall, 1988). Among the 60 capsid proteins, a few, named VP1, have N-terminal extensions (viral protein 1 unique part [VP1up]) that are critical for infection (Hermonat et al., 1984). By transfecting mutants of infectious clones of minute virus of mice (MVM), Tullis et al. (1993) demonstrated that VP1 was dispensable for the production of progeny virus. However, the mutant virus thus obtained was defective during cell entry, subsequent to cell binding but prior to DNA replication.

Cell entry by nonenveloped viruses is still not well understood (Kasamatsu and Nakanishi, 1998). Receptors that have been reported for parvoviruses include globoside for B19 (Brown et al., 1993), human fibroblast growth factor receptor 1, heparin sulfate and $\alpha V\beta 5$ integrin for adeno-associated virus (AAV) (Qing et al., 1999; Summerford et al., 1999), and transferrin receptor for CPV (Parker et al., 2001). Parvovirus internalization involves dynamin-dependent receptor-mediated endocytosis (Parker and Parrish, 1997, 2000), followed by slower intracellular trafficking. Treatments that block the early to late endosomal transport (bafilomycin A1, nocodazole, low temperature) also inhibited virus infection (Vihinen-Ranta et al., 1998; Douar et al., 2001; Hansen et al., 2001), suggesting that transport to the late endosome is required for productive infection. Viral DNA is delivered to the nucleus, either from this endocytic compartment or from the cytoplasm (Parker and Parrish, 2000); however, the molecular mechanisms that regulate nuclear delivery remain unclear.

The role of VP1up in parvovirus entry is essential. Several functions have been attributed to VP1up. VP1up of Aleutian Disease Virus (ADV) parvovirus has DNA binding activity (Willwand and Kaaden, 1988), whereas in other parvoviruses it has been shown to contain nuclear localization signals (Tullis et al., 1993; Vihinen-Ranta et al., 2000). Cotmore et al. (1999) demonstrated that VP1up resides, unexpectedly, within the virion of MVM and is not accessible from the outside. They showed, however, that VP1up can be externalized from intact particles and suggested that this occurs during viral entry.

The VP1up of almost all parvoviruses contains a conserved domain of about 40 amino acids of as yet unknown function. Comparison of this domain from insect parvovirus *Gm*DNV (densovirus from *Galleria mellonella*) with that of porcine parvovirus (PPV) revealed about 90% identity (Tijssen and Bergoin, 1995), while the remainder of their VPs exhibited hardly any similarity (Chapman and Rossmann, 1993; Simpson et al., 1998). Here, we show that some amino acids in the conserved domain of VP1up match critical amino acids in the catalytic site of secretory phospholipase A_2 ($sPLA_2$), an activity that was not known to exist in virus capsids. PLA_2s

[3] Correspondence: peter.tijssen@inrs-iaf.uquebec.ca

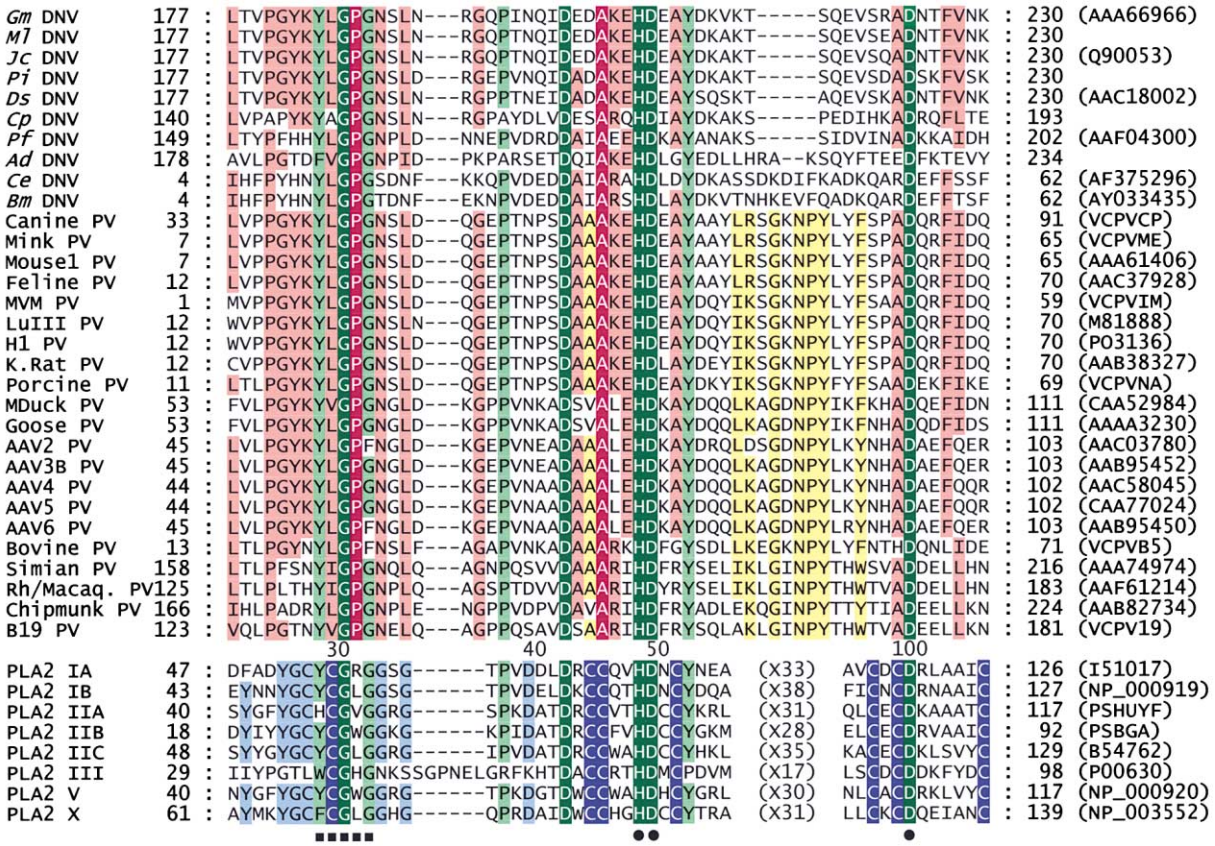

Figure 1. Sequence Alignments of Parvovirus PLA_2 Motifs and $sPLA_2$ Representatives

Parvoviral and $sPLA_2$ sequences with GenBank accession numbers (except those not yet deposited) are separated by the common structural numbering for group I/II $sPLA_2$ (Renetseder et al., 1985). The Ca^{2+} binding loop is underscored by filled squares and the catalytic residues by filled circles. Insect parvoviruses are indicated by DNV and their host name: *Gm*, *Galleria mellonella*; *Ml*, *Mythimna loreyi*; *Jc*, *Junonia coenia*; *Pi*, *Pseudoplusia includens*; *Ds*, *Diatraea saccharalis*; *Cp*, *Culex pipiens*; *Ce*, *Casphalia extranea*; *Ad*, *Acheta domesticus*; *Pf*, *Periplaneta fuliginosa*; *Bm*, *Bombyx mori*. Vertebrate parvoviruses are indicated with PV. K. Rat, kilham rat; MVM, minute virus of mice; Mduck, muscovy duck; Rh/Macaq., rhesus-macaque monkeys; AAV, adeno-assotiated virus. LuIII and H1 parvoviruses originated from tissue cultures, and B19 is a human parvovirus. $sPLA_2$ representatives are indicated by group number: IA, *Naja naja* snake venom PLA_2; IB, human pancreatic PLA_2; IIA, human synovial fluid PLA_2; IIB, gaboon viper snake venom PLA_2; IIC, rat PLA_2; III, bee venom PLA_2; V, human PLA_2; X, human PLA_2. Dark green background (white lettering), 100% identity; light green background, at least 70% conserved among all PLA_2s. Dark and light red indicate 100% identity and at least 70% conserved, respectively, among $pvPLA_2$s. Dark and light blue indicate 100% identity and at least 70% conserved, respectively, among $sPLA_2$s. Yellow background indicates conserved residues in vertebrate parvoviruses [conserved amino acids: (L, V, I), (Y, W, F), (R, K)].

form a superfamily of key enzymes involved in physiological and pathological processes such as lipid membrane metabolism, signal transduction pathways, inflammation, acute hypersensitivity, and degenerative diseases (Dennis, 1997; Kramer and Sharp, 1997; Balsinde et al., 1999). PLA_2s catalyze the hydrolysis of phospholipid substrates at the 2-acyl ester (*sn*-2) position to release lysophospholipids and free fatty acids. Among the major $sPLA_2$ groups, pancreatic $sPLA_2$s from vertebrates and PLA_2s from snake venoms are classified in group I, nonpancreatic and synovial $sPLA_2$s and $sPLA_2$s from crotalid and viperid venoms in group II, and bee venom and related $sPLA_2$s in group III. Members of groups I and II have a similar 3D structure that is different from that of group III (Renetseder et al., 1985). In addition to various physiological roles, $sPLA_2$s are involved in the pathogenesis of inflammation and autoimmune processes (Pruzanski and Vadas, 1991).

In this study, capsids of most parvoviruses were shown to contain this enzyme domain, and this activity was found to be required for parvovirus entry. These findings could provide a basis to study the proposed link between autoimmune disorders and parvovirus infections.

Results

Identification of a Phospholipase A_2 Motif and Activity in the Largest Structural Protein of Parvoviruses

Analysis of 34 parvovirus VP1up sequences revealed that 31 contain a conserved HDXXY motif, found in the catalytic site of $sPLA_2$s (Dennis, 1997). Furthermore, the conserved Ca^{2+} binding loop of $sPLA_2$s, a YXGXG motif (Dennis, 1997), was found in these 31 VP1up sequences (Figure 1). Sequences outside the catalytic site and the

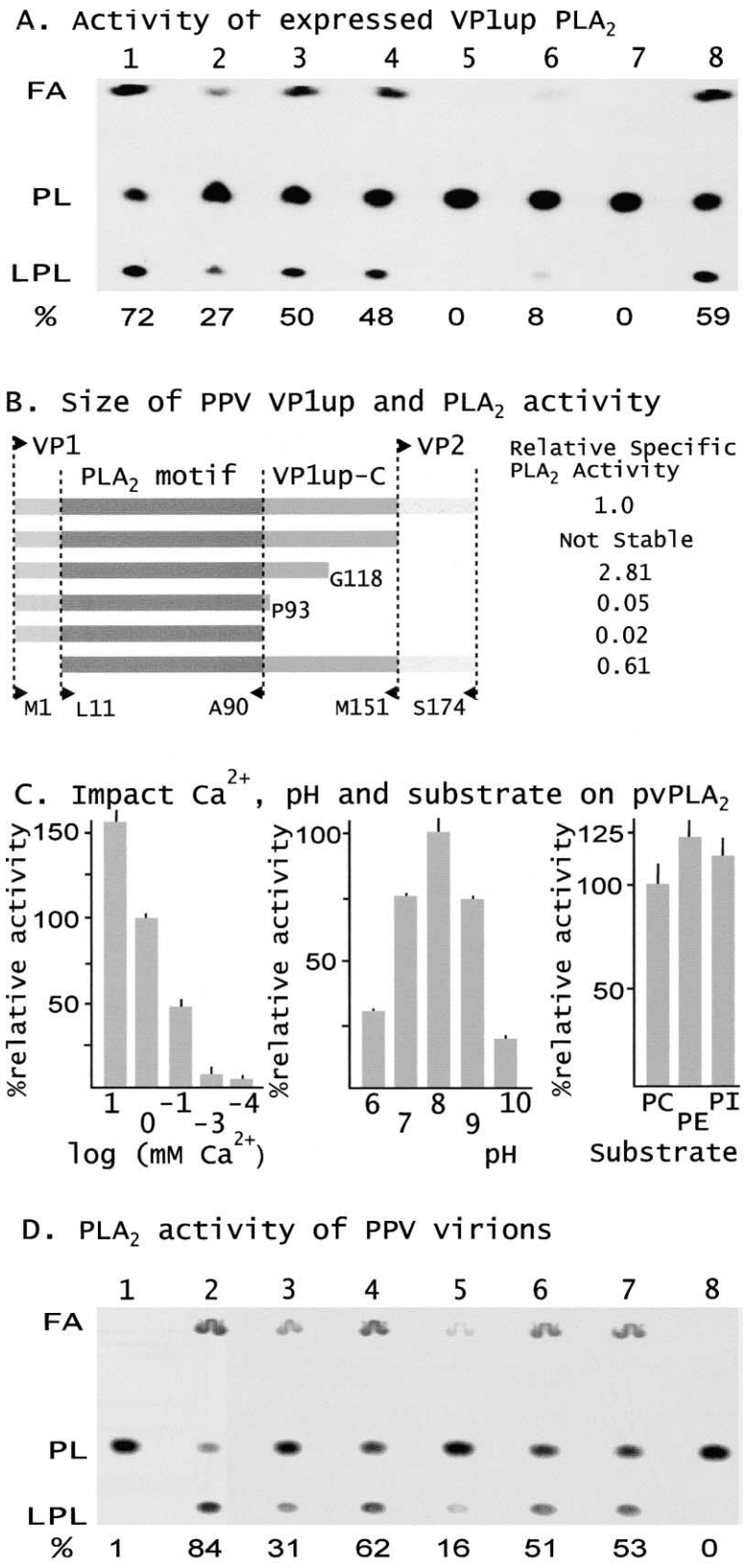

Figure 2. PLA_2 Activity of Viral and Expressed Parvoviral VP1up

(A) Thin-layer chromatography after hydrolysis in the mixed micelles assay of phosphatidylcholine substrate (PL) by expressed $pvPLA_2$ into fatty acid (FA) and lysophosphatidylcholine (LPL). This activity was analyzed with a Molecular Dynamics PhosphorImager [percent: fraction hydrolyzed in percent = ((FA + LPL)/(FA + PL + LPL)) × 100]. PLA_2s used were as follows: lanes 1, 2, and 5 (0.6 ng of PPV PLA_2), lanes 3 and 4 (250 ng of B19 PLA_2), lane 6 (350 ng of *Gm*DNV PLA_2), lane 7 (2,000 ng thioredoxin as negative control), and lane 8 (15 ng bee venom PLA_2). The 3C9 monoclonal antibody, which binds to the C terminus of PPV-VP1up, reduced PPV PLA_2 activity of VP1up (lane 2, 18% of original activity after adding 200 ng of antibody) but not of B19 (lane 4). Adding EGTA to 5 mM abolished PLA_2 activity (lane 5).

(B) Sequences outside the conserved $pvPLA_2$ domain increased $pvPLA_2$ activity of the expressed PPV VP1ups. VP1up from M1 to S174 was used throughout this work and was assigned the relative specific activity of 1.0. Sequences within this expressed peptide but outside the PLA_2 motif (dark gray) contributed to the activity as shown by the relative specific activities.

(C) The impact of Ca^{2+} concentration, pH, and different substrates on the activity of $pvPLA_2$. Since 1 mM Ca^{2+}, 50 mM Tris-HCl, pH 8.0, and phosphatidylcholine (PC) were used in standard assays, these were set at 100% relative activity. PE is phosphatidylethanolamine, phosphatidylinositol (PI). Samples were measured in triplicate.

(D) PLA_2 activity of untreated 0.2 μg virions (lane 1) and after dissociation (lanes 2 and 3) and heat shock (lanes 4 and 5). Bee venom PLA_2 was included as a control at 18 ng (lanes 6 and 7), and lane 8 had a negative control. Samples in lanes 3, 5, and 7 were treated with anti-VP1up antibodies (200 ng). These antibodies reduced viral but not bee venom PLA_2.

Ca^{2+} binding loop motifs are poorly conserved between the putative parvoviral (pv) PLA_2 group and the $sPLA_2$ groups.

VP1up polypeptides from PPV, *Gm*DNV, and B19 parvoviruses were expressed as thioredoxin fusion proteins in order to demonstrate $pvPLA_2$ activity. PLA_2 activity of

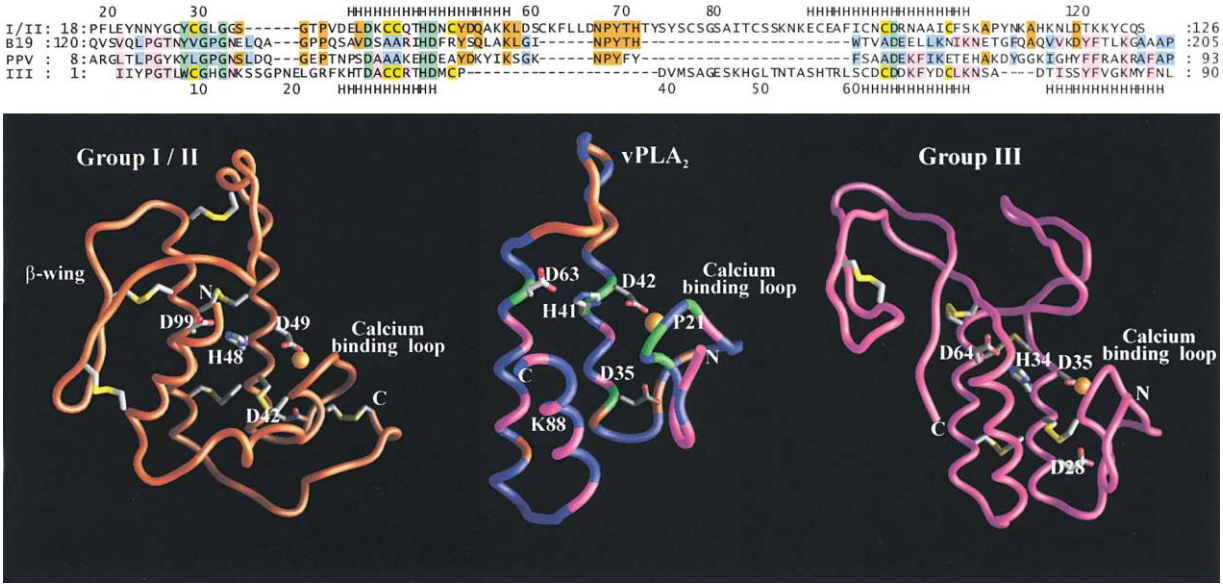

Figure 3. Predicted 3D Structure of PPV/B19 pvPLA$_2$ Domain

Sequences of PPV/B19 showed homology with the N and C termini of group III sPLA$_2$ and with the middle part of group I/II sPLA$_2$ (IB pancreatic sPLA$_2$; GenBank accession numbers in Figure 1). Helices are indicated by stretches of H. The predicted 3D model of B19/PPV PLA$_2$ has been obtained by homology modeling using the program MOE. Both the 3D structure of pancreatic porcine PLA$_2$ (Group I/II in orange; PDB number 1P2P) and bee venom PLA$_2$ (Group III in magenta; PDB number 1POC) were used for homology modeling of pvPLA$_2$ (in the middle). Residues L, V, I as well as residues Y, F, W were considered equivalent residues. It was assumed that disulfide bridges are not essential for the structure since mutations of cysteine did not affect enzyme activity (Zhu et al., 1995). The 3D images were generated with the program GRASP. The color code in the sequence matches that in the pvPLA$_2$ structure. The green color in pvPLA$_2$ indicates residues that are conserved with both group I/II and group III PLA$_2$s, orange-coded residues are conserved with group I/II, and magenta-coded are conserved with group III PLA$_2$s. Amino acids labeled in the pvPLA$_2$ structure were submitted to site-directed mutagenesis.

purified VP1up was measured with the mixed micelles assay (Manjunath et al., 1994). The thioredoxin alone did not exhibit any PLA$_2$ activity (Figure 2A) and served as a control. The catalytic efficiency $(k_{cat}/K_M)_{app}$ of expressed PPV PLA$_2$ was (71.9 ± 9.4) × 10^5 $M^{-1}{\cdot}s^{-1}$ compared to (1.09 ± 0.14) × 10^5 $M^{-1}{\cdot}s^{-1}$ for bee venom sPLA$_2$. The $(k_{cat}/K_M)_{app}$ of B19 and *Gm*DNV PLA$_2$ were (2.5 ± 0.2) × 10^4 and (0.4 ± 0.03) × 10^4 $M^{-1}{\cdot}s^{-1}$, respectively. Extended regions of PPV VP1up, each containing the conserved pvPLA$_2$ domain, were expressed, and activity determinations indicated that sequences outside the conserved domain had a large impact on the catalytic efficiency of the enzyme (Figure 2B).

Monoclonal antibody (3C9; ATCC CRL-1745) specific to the C terminus of the PPV-VP1up reduced the PLA$_2$ activity of PPV, but not that of B19 (Figure 2A). sPLA$_2$ inhibitors oleyloxyethylphosphorylcholine (OP) and manoalide (MA) also inhibited the VP1up PLA$_2$ activity. The MA concentration for 50% inhibition (IC_{50}) in the radiolabeled *E. coli* PLA$_2$ assay was 3.8 ± 0.4 μM and 2.0 ± 0.3 μM for B19 and PPV PLA$_2$, respectively. The IC_{50} for OP was >20 μM for B19 and 11.1 ± 0.9 μM for PPV PLA$_2$. The pH optimum of PPV PLA$_2$ in the mixed micelles assay was 8.0 (Figure 2C). The Ca^{2+} concentration for optimum activity of this expressed PPV PLA$_2$ was slightly above 10 mM (Figure 2C), as for most sPLA$_2$, whereas chelating Ca^{2+} by EDTA or EGTA abolished activity of both PPV and B19 pvPLA$_2$ (Figure 2A).

PPV and B19 pvPLA$_2$ did not exhibit a substantial substrate preference among phosphatidylcholine, -ethanolamine, and -inositol phospholipids when determined by the mixed micelles assay (Figure 2C). Since the phosphatidylethanolamine and -inositol substrates were labeled only at the *sn*-2 position, fatty acids but not lysophospholipids could be detected after the reaction. In contrast, phosphatidylcholine was labeled at both *sn*-1 and *sn*-2 positions, and both fatty acid and lysophospholipid products were detected with the PhosphorImager. These data confirmed pvPLA$_2$ as a new member of the PLA$_2$ enzyme family.

PLA$_2$ activity in purified virus was only detected when PPV virions were assayed at high concentrations (>4 μg/ml), suggesting that PLA$_2$ domains reside inside the intact capsid as shown for MVM (Cotmore et al., 1999). This was confirmed since disruption of the capsid by alkali denaturation and renaturation, thereby exposing the VP1up, increased the PLA$_2$ activity 50- to 100-fold, close to levels of expressed VP1up (Figure 2D). A heat shock of 2 min at 70°C also released VP1up as the PLA$_2$ activity increased about 20–50 times (Figure 2D). PLA$_2$ activity of PPV VP1up, exposed after dissociation of capsids or by heat shock, but not that of bee venom PLA$_2$, was significantly reduced by polyclonal antibodies raised against PPV VP1up (Figure 2D), demonstrating that under specific conditions virion-associated PLA$_2$ activity can be revealed.

Site-Directed Mutagenesis of Critical Amino Acids in the Phospholipase A$_2$ Domain and Effect on Enzyme Activity and Viral Infectivity

The 3D structure of many group I/II and group III sPLA$_2$s has been solved (e.g., Dijkstra et al., 1981; Renetseder et al., 1985; Dennis, 1997; Sekar and Sundaralingam,

Table 1. Impact of Mutations in $pvPLA_2$ of PPV on Enzyme Activity and Infectivity

$pvPLA_2$ Mutants (PPV)	Position in Group I/II	Position in Group III	Relative Specific Activity (%)	Relative Specific Infectivity (%)
wt	—	—	100	100
P21L	31	11	7.5	0.62
P21R	31	11	0.07	0.0012
P21W	31	11	4.1	0.055
D35E	42	28	0.27	0.071
D35N	42	28	0.02	0.0019
H41A	48	35	<0.007	0.0011
D42N	49	36	0.04	0.0012
HD41/42AN	48/49	35/36	<0.005	0.0011
D63A	99	64	<0.003	0.0003
D63N	99	64	0.05	0.0007
K88R	—	85	0.01	0.0035

Hydrolysis of the substrate was measured, as shown in Figure 2, with a PhosphorImager. The specific activity of mutant enzymes were compared to that of wt PPV $pvPLA_2$. The infectivity of wild-type (wt) and mutant viruses was measured by the number of full particles, as established by genome equivalents in the quantitative PCR (MIMIC) assay, required to obtain one fluorescent focus upon infection, after comparing to wt. Dilutions were used that gave at least 25 fluorescent focus units (ffu) (relative error < 0.2). For wt PPV, 232 full particles were required per fluorescent focus. The relative specific infectivity of mutants is as compared to wt results (five independent assays). The correlation coefficient between the enzyme activity and viral infectivity, r^2, was 0.898 (excluding K88R, which may be outside the PLA_2 domain).

1999) and served to predict the B19/PPV $pvPLA_2$ structure (Figure 3). Potentially critical amino acids could thus be targeted for site-directed mutagenesis (Weiner et al., 1994) at positions indicated in Figure 3. Transfection of susceptible cell lines by the infectious clone of PPV yields wild-type (wt) virus (Bergeron et al., 1996). Site-directed mutagenesis of the infectious clone prior to transfection enabled us to obtain defined mutant viruses. These defined mutations made it possible to study the relationship between $pvPLA_2$ activity and virus infectivity.

Both enzyme activity and viral infectivity decreased dramatically when amino acids in the catalytic site ($H41^{pv}$ and $D42^{pv}$) were mutated (Table 1). (Positions in $pvPLA_2$ are those of PPV VP1 and are distinguished from $sPLA_2$ positions by adding the superscript pv.) $D63^{pv}$ was conserved in $pvPLA_2$ suggesting that it corresponded to the catalytic D99 in $sPLA_2$ (Figure 1). Its replacement by $A63^{pv}$ or $N63^{pv}$ decreased strongly both enzyme activity and viral infectivity, supporting the predicted relative position of α helices in the 3D-structural model (Figure 3). Site-directed mutagenesis of $D35^{pv}$, conserved among both $sPLA_2$ and $pvPLA_2$, to $D35^{pv}E$ and $D35^{pv}N$, also strongly reduced enzyme activity and infectivity (Table 1). $P21^{pv}$ was conserved in the Ca^{2+} binding loop of all $pvPLA_2$ but not among that of $sPLA_2$. When $P21^{pv}$ was mutated to amino acids that occur often at that position in $sPLA_2$ (R, W, L), both the enzyme activity and the infectivity were significantly reduced (Table 1). The role of the $K88^{pv}$, which is conserved in parvoviruses and bee venom PLA_2, is unknown but essential as even conservative mutagenesis ($K88^{pv}R$) strongly lowered activity. Overall, the impact of mutations showed a correlation ($r^2 = 0.898$) between enzyme activity and viral infectivity of the viral mutants (Table 1).

Viral Phospholipase A_2 Is Required for Infection

As described above, both wt and PLA_2 mutant infectious clones were effective in producing virions upon transfection. Hence, $pvPLA_2$ is required before replication and packaging. Conversion of single-stranded parvoviral genomes into double-stranded DNA during normal infection is achieved in the nucleus by cellular DNA polymerase (Tattersall and Cotmore, 1990). Therefore, pvPLA2 is implicated in the infection process prior to the presence of single-stranded genomes in the nucleus.

To test the hypothesis that $pvPLA_2$ acts on entry into the cell, wt, $P21^{pv}W$, and $HD41^{pv}/42^{pv}AN$ mutants of PPV were labeled with [^{35}S]methionine and the relative efficiency of binding and entry was determined. Binding and entry assays showed that $pvPLA_2$ mutations did not influence infectivity at these stages (Figures 4A and 4B).

After entry into the cells, both wt and mutant viruses accumulated within perinuclear vesicular structures as early as 2 hr after infection. Colocalization of internalized virus with the major lysosomal glycoprotein, LAMP-2, was quite extensive (Figure 5A) and identified the endocytic organelle to which PPV is delivered as a late endosome or lysosome (Griffiths et al., 1988; Geuze et al., 1988). The extent of colocalization of mutants with LAMP-2 was similar to that of wt (Figure 5A). PPV capsids, expressed in the baculovirus system and lacking VP1up altogether, also colocalized with this marker and indicated that $pvPLA_2$ is not required for traffic of PPV to the late endosome/lysosome (Figure 5A). Incoming capsids of both wt and mutant viruses remained in the late endosomal/lysosomal compartments and egress of viral capsids to the cytoplasm was not observed.

Inhibitors of $sPLA_2$, tetracaine, and OP were used to confirm that PLA_2 activity controls viral infectivity by facilitating lysosome-to-nucleus transport of the viral DNA. In order to reduce the infectivity at 20 hr to 50%, as measured by the number of fluorescent foci, the required concentration was 34.6 ± 2.8 μM for tetracain and 13 ± 2.1 μM for OP. Nuclear delivery of the viral genome was essentially blocked at 12 hr and significantly reduced at 16 hr postinfection, demonstrating that PLA_2 activity is required for PPV infectivity (Figure 4D). In the presence of PLA_2 inhibitors, wt virus was predominantly localized to the late endosome/lysosome compartment (data not shown). Thus, studies with both PLA_2 mutants and PLA_2 inhibitors demonstrated that PLA_2 activity is required by the viral genome for its transfer from the late endosomal/lysosomal compartment to the nucleus.

To establish whether infectious DNA and active

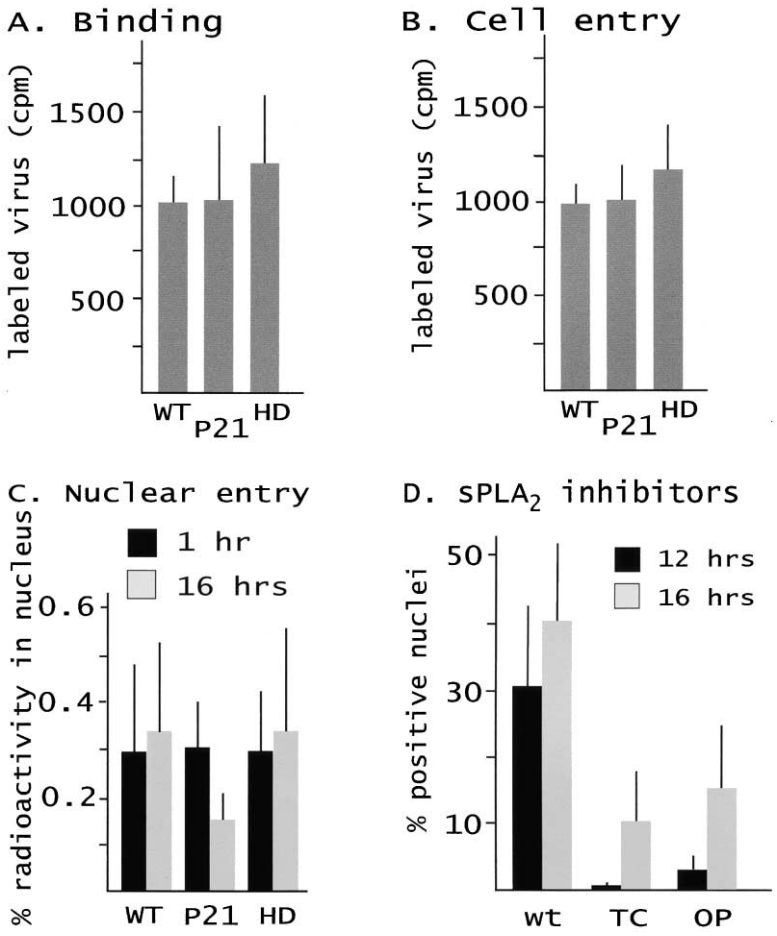

Figure 4. Parvoviruses Did Not Require pvPLA$_2$ Activity for Binding to the Cell Surface or Initial Stages of Entry

(A and B) Binding (A) and entry (B) of ^{35}S-labeled PPV were studied using 4×10^5 cells and 5×10^9 wt particles and equivalent amounts of mutant viruses for binding and twice as many for entry (experiments in quadruplicates). Viruses bound either to cells or entered into cells were measured by a liquid scintillation method after performing the washing or antibody-stripping procedures, respectively. pvPLA$_2$ mutations had no effect on virus binding to the cells or entry. Both binding and entry of virus were time and dose dependent (data not shown).

(C) ^{35}S-labeled PPV particles (10^6 cpm) (wt and mutants) were added to 2×10^7 cells in petri dishes, and about 20% was recovered in the cells. After cellular fractionation, the distribution of virus over cytosolic and nuclear fractions was measured by liquid scintillation. The relative radioactivity is calculated by the following: (nuclear fraction-bound activity)/(cellular fraction-bound activity). Standard errors are calculated from three experiments. Few or no capsids penetrated the nucleus, despite the large amount of virus that entered the cells.

(D) sPLA$_2$ inhibitors tetracain (TC), at 10 μM, and oleyloxyethylphosphorylcholine (OP), at 20 μM, also reduced the number of nuclei with viral DNA, as detected by in situ DNA hybridization.

pvPLA$_2$ needed to reside in the same particle to be infectious, complementation studies were undertaken. The addition during infection of 1 μM expressed wt pvPLA$_2$ or 0.4 μM snake or bee venom sPLA$_2$ in *trans*, at a 10^4-fold excess to PLA$_2^-$ virus mutants, could not rescue the virus (data not shown). Wt virus with β-propiolactone-inactivated DNA (infectivity decreased >100,000-fold), but active pvPLA$_2$ (70% activity of untreated) in a 10-fold excess, also failed to rescue mutant virus upon coinfection. Active pvPLA$_2$ and infectious DNA is therefore required in *cis* to obtain infection.

Role of Viral Phospholipase A$_2$ during Infection

A critical role for viral delivery to the late endosome/lysosome in viral infectivity was demonstrated by the fact that adding the lysosomotropic base NH_4Cl prior to infection reduced viral infection in a dose-dependent fashion (5, 20, and 50 mM decreased PPV infectivity by 82%, 99% and 99.92%, respectively) and also exacerbated the effect of the mutations by delaying infectivity and lowering the number of fluorescent foci even further (Figure 5B).

De novo viral antigen was detected in the nucleus by immunofluorescence from about 8–12 hr postinfection with wt PPV (Figure 5B) but only after at least 18 hr and in far fewer nuclei for mutant virus (Figure 5B; Table 1). In order to selectively follow incoming wt virus at late stages of infection, without interference of newly synthesized PPV protein, PPV infection was performed under conditions where protein synthesis was blocked. In the presence of cycloheximide, at 10 μg/ml, incoming virus particles were not detected in the nucleus (data not shown). The inability of incoming wt and mutant viral capsids to access the nucleus was confirmed by the lack of traffic of ^{35}S-labeled capsids to the nucleus. In this experiment, about 10^6 cpm of labeled virus (wt, P21^{pv}W, and HD/AN mutants) were added, and the import of radiolabel into the nuclear fraction was assessed at 1 and 16 hr after infection. While 2×10^5 cpm of labeled virus entered the cells, the amount of cpm in the nuclear fraction remained constant over this period at <0.5% (Figure 4C), essentially equivalent to the extent of cytosolic contamination of the nuclear fraction as measured by lactate dehydrogenase activity (<0.5%). Relative to the large quantity of virus that entered the cells, little or no virus-associated protein penetrated the nucleus.

In situ DNA hybridization was undertaken to investigate whether mutant viruses transferred their genome from the late endosomal/lysosomal compartment to the nucleus as efficiently as wt PPV. At 4 and 8 hr, viral DNA was detected in the perinuclear late endosomal/lysosomal compartments, whereas wt viral DNA replication started in the nucleus prior to 12 hr postinfection

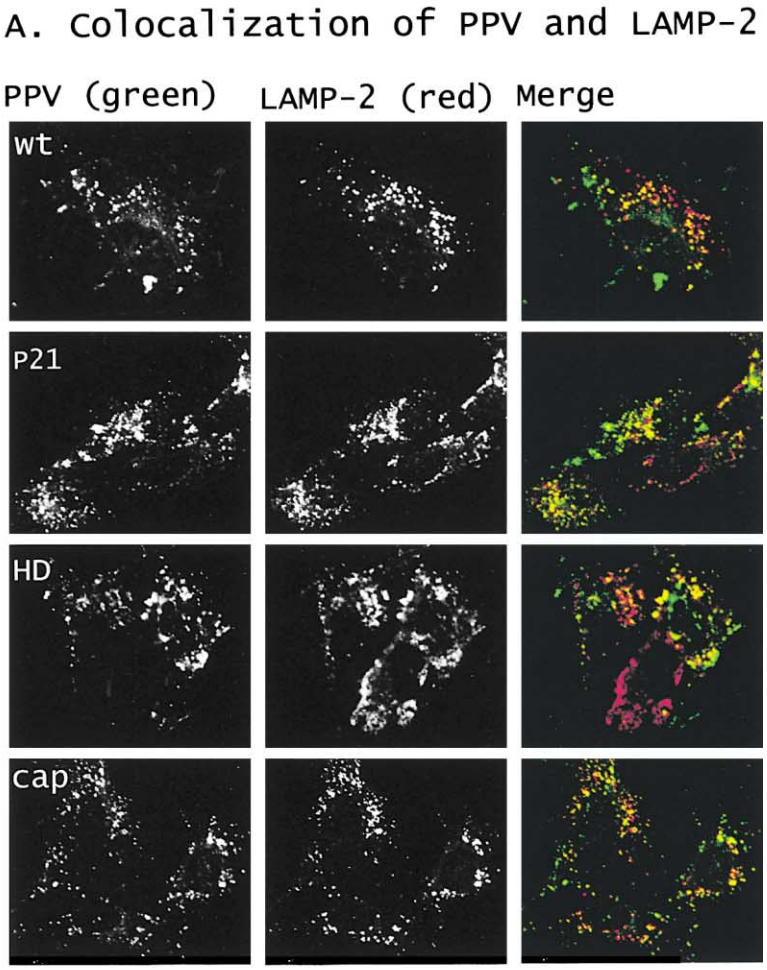

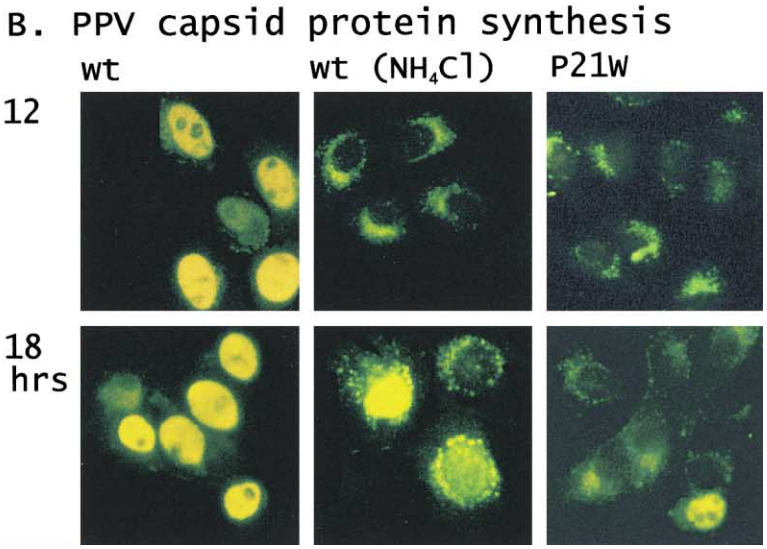

Figure 5. Incoming PPV Capsids Target Late Endosomes/Lysosomes

(A) Colocalization of PPV and LAMP-2 was studied by confocal microscopy. Anti-PPV antibodies were labeled with FITC, giving green fluorescence, and anti-LAMP-2 antibodies with Texas red, giving red fluorescence. Colocalization of PPV and LAMP-2 resulted in yellow staining. Both wt and mutants as well as capsids lacking PLA_2 showed extensive colocalization with LAMP-2 in the late endosomes/lysosomes.

(B) Immunofluorescence (anti-PPV antibodies) was used to follow the entry and infection of PT cells by wt or mutant virus (concentration of 0.5 μg/ml), with or without 20 mM NH_4Cl. After 12 hr, both P21W mutant virus and wt virus in the presence of NH_4Cl were perinuclear. In the absence of NH_4Cl, wt virus infected many cells as indicated by the presence of positive nuclei. This was the result of synthesis of new capsid proteins, as in the presence of cycloheximide (10 μg/ml) no positive nuclei were observed (data not shown). After 18 hr, few positive nuclei were detected with the P21W mutant or with wt virus in the presence of NH_4Cl.

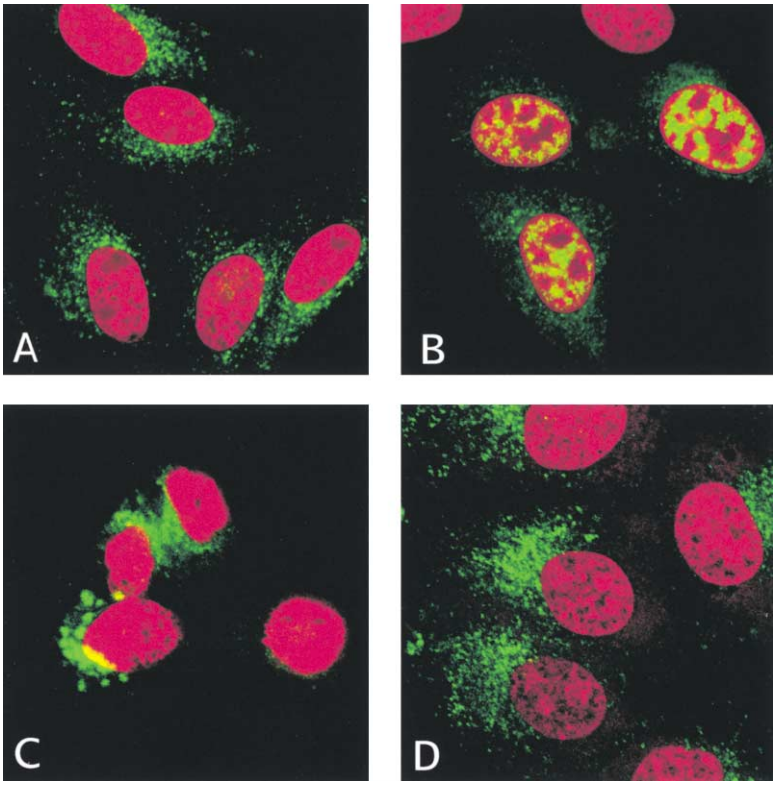

Figure 6. Distribution of Viral DNA in Infected Cells

Using in situ hybridization, incoming viral DNA was detected in the cytoplasm after 4 (data not shown) and 8 (A) hr, whereas replicating viral DNA was found at 12 hr postinfection (B). At this stage, viral DNA could not be detected in the nucleus in the case of the HD/AN mutant, lacking pvPLA$_2$ activity (C), or with the P21^{pv}W mutant, which has weak PLA$_2$ activity (D).

(Figures 6A and 6B). The inability to detect DNA of the HD and P21 mutants at the same time in the nucleus (Figures 6C and 6D) suggested that DNA from mutant virus did not penetrate the nucleus, since incoming viral DNA would be replicated rapidly to detectable amounts by the host cell machinery. In conclusion, PLA$_2$ mutants are strongly impaired in the transfer of the viral genome from the perinuclear vesicles into the nucleus.

Discussion

The pvPLA$_2$s Are a Subgroup in the PLA$_2$ Superfamily

The conserved VP1up domain of parvoviruses is shown here to exhibit a PLA$_2$ activity that is essential for parvovirus infectivity. pvPLA$_2$s and sPLA$_2$s share a conserved Ca^{2+} binding loop and catalytic site. The pvPLA$_2$s differ from sPLA$_2$s as follows: (1) cysteine is absent from all VP1up pvPLA2 sequences, whereas all sPLA$_2$s are disulfide-rich; (2) the connecting sequence between the two helices containing the catalytic site (D63^{pv} and H41^{pv}) is much shorter in pvPLA$_2$ than in sPLA$_2$ (D99 and H48); and (3) P21^{pv} in the YXGPG sequence in the Ca^{2+} binding loop of all pvPLA$_2$ is strictly conserved, in contrast to that of sPLA$_2$. In view of the differences with sPLA$_2$, such as structure (Figure 3), biological role, and unique sequences (Figure 1), we propose that pvPLA$_2$s form a new group within the PLA$_2$ superfamily, which we refer to as group XIII.

Molecular modeling of pvPLA2 suggests that the shorter loop connecting the H41^{pv} and D63^{pv} helices cannot shield the catalytic D63^{pv} from the aqueous phase as the β-wing does with D99 of the group I/II/V/X sPLA$_2$s (Figure 3). This deficiency may be compensated for by other structures in the viral capsid and sequences outside the conserved PLA$_2$ domain. The increased enzyme activity obtained after expression of extended PLA$_2$ domains supports this hypothesis and also corroborates the proposed structural resemblance of the pvPLA$_2$ with those from group III (Figure 3). The N-terminal helix in group I/II/V/X sPLA$_2$s is upstream of the Ca^{2+} binding loop and binds to the interface (Gelb et al., 1999). However, this helix is predicted to be downstream of the catalytic site in pvPLA$_2$, as in group III sPLA$_2$. This projection by molecular modeling is supported by (1) the minor impact on enzyme activity caused by a truncation upstream of the Ca^{2+} binding loop and (2) the absence of extra sequences upstream of the Ca^{2+} binding loop in some parvoviruses (immunosuppressive MVM, *Bm*DNV; Figure 1).

In sPLA$_2$, H48 functions as a general base and is assisted by D99 to deprotonate a catalytic water molecule that hydrolyzes the phospholipid ester (Dennis, 1997). The adjacent D49, via its β-carboxyl group, and backbone carbonyl oxygens from Y28, G30, and G32 in the Ca^{2+} binding loop coordinate the catalytic Ca^{2+} cofactor involved in the stabilization of the transition state (Dennis, 1997; Murakami et al., 1997; Dessen, 2000). The observation that D35^{pv}/D42 is strongly conserved among all pv/sPLA$_2$ indicated that this residue has an essential role. Mutation of this residue was poorly tolerated (Table 1). The 3D structures suggest that D35^{pv}/D42 is critical for the positioning of the Ca^{2+} binding loop, with respect to the active site, by three hydrogen bonds.

The catalytic efficiencies of pvPLA$_2$s, as expressed by $(k_{cat}/K_M)_{app}$, were within the 1–2 log range of that of

bee venom PLA_2. These differences may be due to the assay system or the cloning of incomplete active domains for expression but could also reflect real differences. Large activity differences are common among $sPLA_2$s and have been attributed to variations in strength of the interfacial contacts with the substrate (Han et al., 1999). The high catalytic efficiency of PPV PLA_2 may be due to a prolonged stay at the interface and to a scooting mode of hydrolysis.

pvPLA$_2$ Activity Is Required for Viral Infection

The correlation between enzyme activity and virus infectivity underscores the essential role of this enzyme during infection. Data obtained with transfection of wt or mutant infectious clones established that $vPLA_2$ acts prior to viral replication and expression. Little is known about mechanisms underlying the early steps of parvovirus infection. The demonstrated delivery of PPV to LAMP-2 positive late endosomes/lysosomes confirms that PPV enters the cell via the classical endocytic pathway, consistent with other parvoviruses (Vihinen-Ranta et al., 1998; Duan et al., 1999; Parker and Parrish, 2000). Colocalization studies with LAMP-2, using confocal microscopy, showed that both wt and mutant viruses are rapidly delivered to the late endosome/lysosome, by about 2–4 hr, and that incoming capsids remained in this location. Capsids that lack VP1up, and consequently $pvPLA_2$, also reached these perinuclear organelles and could not be distinguished from wt. Therefore, $pvPLA_2$ is not required for attachment to the cell surface, early stages of endocytosis, or the transfer of virus to late endosomes.

The position of VP1up inside the capsid prior to endocytosis was confirmed in this study for PPV as $pvPLA_2$ was detected in dissociated capsids but hardly in intact capsids. Moreover, antibodies to VP1up do not bind to virus in ELISA assays (data not shown). The *cis* requirement of $pvPLA_2$ for productive infection and complementation studies showing that wt $pvPLA_2$ cannot rescue PLA_2-negative mutants also demonstrate the critical role of $pvPLA_2$ in viral infectivity. To implement its critical role during entry, PLA_2 should gain access to the cellular environment. Externalization of VP1up from intact particles can be achieved in vitro (Cotmore et al., 1999) but is accompanied by a conformational transition so that the viral genome becomes susceptible to externally applied DNase. Treatment of MVM parvovirus with extracts from susceptible cells, but not from nonsusceptible cells, also rendered the viral genome accessible to DNase (Previsani et al., 1997). This suggests that susceptible cells contain a factor that destabilizes the virion and may be required for the externalization of VP1up. The absence of disulfide bridges in $pvPLA_2$, in contrast to all known $sPLA_2$, would facilitate this externalization through the cylindrical channel at the 5-fold axis of the capsid. In contrast to the loop 3 and 4 polypeptide chains around the 3-fold axis, the subunits are not interwoven at the 5-fold axis and the capsid may open further around the 5-fold cylinder during this process. Externalization would expose the $pvPLA_2$ group only when essential, together with other VP1up functions (DNA binding, nuclear localization) that may be required in a coordinated fashion for endosome exit and viral genome transfer. The acidic lysosomal milieu may facilitate conformational changes of the viral capsid and consequent externalization of the VP1up. Shielding of small amounts of externalized pvPLA2 from the acidic lumen, perhaps via membrane interaction, may enable $pvPLA_2$ activity and viral egress. Expression of active PLA_2 by a small subset of virions could explain the apparent inefficiency of lysosome-to-nucleus delivery and viral infectivity described here.

In situ hybridization studies showed that $pvPLA_2$ mutations as well as inhibition of PLA_2 activity affected the transfer of the viral genome to the nucleus. Incoming mutant as well as wt virus capsids accumulate in perinuclear lysosomal compartment over extended time periods. In contrast, incoming AAV particles can be detected in the nucleus from about 3 hr postinfection (Sanlioglu et al., 2000). VP1up of AAV is large and probably localized on the outside of the particle, like that of *Gm*DNV and B19 (Rosenfeld et al., 1992), and thus may not require this VP1up externalization step, leading to a different genome delivery mechanism via intact particles.

The outside location of B19-VP1up (Rosenfeld et al., 1992) and its phospholipase domain could explain the presence of antiphospholipid-protein complex antibodies in B19-related syndromes such as SLE (Loizou et al., 1997), and the specific expression of B19 VP1 in the synovia of RA patients (Takahashi et al., 1998b) could contribute to the high PLA_2 activity in the synovial fluid. The requirement of $pvPLA_2$ for virus infectivity and the differences between $pvPLA_2$ and $sPLA_2$ sequence profiles make this viral enzyme an obvious target for designing a new class of specific antiviral drugs that act via $pvPLA_2$ inhibition.

Experimental Procedures

Vectors, Infectious Clones, and Site-Directed Mutagenesis

The pN2 infectious clone of PPV was derived from the pPPV2/17 clone (pUC19 with the genome of PPV NADL-2 inserted in its SmaI site; Bergeron et al., 1993) by deletion of a vector fragment from 2617 via 2686/0 to 410 (KpnI) to render several restriction sites in the PPV insertion unique. Mutants of this clone were obtained by site-directed mutagenesis (Weiner et al., 1994) of the pVPi clone (pBluescriptIISK$^-$, containing PPV sequence 2287–3664) and then replacing the KasI-EcoRI fragment in pN2 by the corresponding fragment from pVPi. For expression studies, the pBADTBX vector was constructed from the pBAD/TOPO Thiofusion expression vector (Invitrogen) by inserting downstream of the thioredoxin gene a TEV protease site followed by a polylinker (BglII, EcoRI, SfuI, XhoI, SstI, XbaI). The vector contains the sequence for a His-tag downstream of this sequence.

Preparation of Virus and Transfection with Infectious Clones

The PT cell line (Bergeron et al., 1996) was used for all PPV infection experiments and was maintained in Dulbecco's modified Eagle's medium (DMEM) supplemented with penicillin (100 IU/ml), streptomycin (50 μg/ml), and 8% fetal calf serum (HyClone). Semiconfluent monolayers were used for infection. For wild-type (wt) virus, cytopathic effects were observed 3–5 days after infection. Virus was collected from the medium by ultracentrifugation and the pellet was redissolved in a small volume of PBS. After a DNase and trypsin treatment, the virus was further purified by differential centrifugation followed by sucrose gradient centrifugation. For transfection, the undigested pN2Δ clone or its mutants were introduced into PT cells to obtain virus using the Lipofectamine-plus kit (GIBCO-BRL) according to the supplier's recommendations. For mutant clones, two additional infection passages served to monitor for possible revertants.

Preparation of PPV Recombinant Capsids

To produce viral capsids without VP1up, the PPV VP2 coding region (2810–4549) was cloned into BamHI-XbaI sites of the pFastbac baculovirus transfer vector and recombinant baculovirus was generated according to the supplier's recommendations (GIBCO-BRL). High Five cells (InVitrogen) were infected with 5 MOI of VP2-expressing recombinant baculovirus and harvested after 72 hr. Cells were lysed with 1% trypsin, and the lysate was concentrated and washed twice with one vol 0.1 M $NaHCO_3$ (pH 8.6) in Centricon plus-80 filters (100,000 MW cutoff). Concentrated recombinant VP2 capsids were then purified by centrifugation on two successive 20% sucrose gradients and on a CsCl gradient and dialyzed.

Phospholipase A_2 Expression and Activity

The following VP1up domains were cloned in expression vectors: PPV-VP1up amino acid 2–174, B19-VP1up amino acid 2–240, *Gm*DNV-VP1up amino acid 1–378. VP1up was amplified by PCR using primers containing the BglII and XbaI restriction sites, respectively. The amplicons were cloned into BglII-XbaI of the pBADTBX vector, and the clones were sequenced. Correct clones were then used to transform *E. coli* BL21-CodonPlus(DE3)-RIL (Stratagene) to obtain a fusion protein. This protein was purified on a Ni-agarose column. SDS-PAGE and Coomassie blue staining revealed a single band. This protein could be cleaved by TEV protease to remove the thioredoxin. PLA_2 activity of the protein was not significantly affected by the presence of thioredoxin. PLA_2 activity of expressed VP1up was established using the mixed micelles assay (Manjunath et al., 1994) or the *E. coli* radioactive assay (Elsbach and Weiss, 1991). For the mixed micelles assay, the substrates (from New England Nuclear/DuPont) were 6 μM L-3-phosphatidylcholine,1,2-di[1-^{14}C]oleoyl (specific activity 110 mCi/mmol), L-3-phosphatidylinositol L-1-stearoyl-2-[1-^{14}C]arachidonyl (specific activity 48 mCi/mmol), or phosphatidylethanolamine L-1-palmitoyl,2-[1-^{14}C]arachidonyl (specific activity 54.6 mCi/mmol), and the assay was modified in the following way: 1 mM Triton X-100 was used instead of deoxycholate; the reaction total volume was 50 μl and was stopped after 10 min by adding 80 μl chloroform/methanol (2:1) and 50 μl of saturated KCl solution. Separation was on silica gel thin-layer chromatography plates. Optimal separation of the phosphatidylcholine reaction products was obtained using a solvent solution containing chloroform, methanol, and water (65:35:4). For phosphatidylethanolamine and phosphatidylinositol, chloroform and methanol (87:13) were used as solvent. The separated products were quantified using a Molecular Dynamics PhosphorImager SI after drying. Bee venom PLA_2 was purchased from Sigma-Aldrich (cat. no P9279) at 1360 U/mg. Only the regression lines of activity versus dilution with a correlation coefficient $r^2 > 0.98$ were used to calculate the amount of protein to hydrolyze 50% of the substrate in the mixed micelles assay. Alternatively, the first-order rate constant, k, was determined from reaction progress curves using an integrated first-order rate equation ($[P] = S_0(1 - e^{-kt})$ (P is product and S is substrate concentration) in which $k = (k_{cat}/K_M)_{app}E_0$ and E_0 the total enzyme concentration.

Phospholipase Activity in Virions

Activity was determined with purified virus prior to and after dissociation of the capsids or a heat shock. For dissociation of capsids, virus in 50 mM Tris-HCl buffer, pH 8.0, was treated by adding NaOH to 0.05 N and, after 5 min at room temperature, neutralized with 0.1 N HCl. Heat shock was 2 min at 70°C followed by gradual cooling.

MIMIC PCR, Immunofluorescence, and In Situ Hybridization

The concentration of full virus particles, expressed as genome equivalents per microliter, was measured by a MIMIC quantitative PCR assay (Haberhausen et al., 1998), and the concentration of infectious virus was determined by immunofluorescence 20 hr after infection (fluorescent focus units [ffu] per microliter). Primers used for MIMIC PCR were (positions 836–862 in NADL-2) 5′-AGTGGG TATCGCTACTAACCTACACTC and (positions 1207–1181 in NADL-2) 5′-GATCTGTCATCATCCAGTCTTCTATGC. The competing MIMIC amplicon contained a deletion from positions 863–903 and was cloned into a pBluescript plasmid. Quantification of full virus particles (GE) with the MIMIC method was repeated until the coefficient of variation was less than 0.3. For immunofluorescence, the 3C9 monoclonal antibody (ATCC CRL-1745) was used. Virus was diluted so that at least 25 ffu were counted and the relative error in the estimates of ffu/ml would be <0.2.

The double labeling of internalized PPV with LAMP-2 was performed using a porcine polyclonal anti-PPV antibody and the AC17 mouse anti-canine LAMP-2 monoclonal antibody (Nabi et al., 1991; Nabi and Rodriguez-Boulan, 1993) that has previously been reported to recognize mink LAMP-2 (Hariri et al., 2000). Appropriate controls were performed to ensure that the antibody labeling was specific. In situ hybridization was performed using DIG-conjugated anti-VP1 and anti-NS1 probes and FITC-conjugated anti-DIG antibody sandwich labeling according to the manufacturer's instructions (Roche Molecular Biochemicals). Nuclear labeling was performed by the addition of 0.02 mg/ml propidium iodide to paraformaldehyde-fixed cells after labeling. Confocal images were acquired using the 63× PlanApochromat objective of a Leica TCS SP confocal microscope equipped with argon and krypton laser sources.

Effect of Viral Phospholipase A_2 Mutations during Binding or Entry into the Cells

The binding of virus to cells was measured by scintillation counting after adsorption of ^{35}S-labeled particles to the cells at 4°C and washing. In detail, metabolic labeling of virus with ^{35}S was achieved as follows: wt pN2 as well as its P21W and HD mutants were transfected into PT cells in 6-well plates (1 μg DNA/well) using the Lipofectamine-plus kit (GIBCO-BRL). The medium was changed after 12 hr to methionine-free medium. After an additional hour, [^{35}S]methionine (60 μCi/ml) was added in fresh methionine-free medium to the cells. After a further 12 hr incubation period, 2 ml regular medium (8% fetal bovine serum [FBS] in DMEM) was added to the cells and virus was purified 60 hr after transfection. Binding to cells was measured as follows: about 10^4 cpm [^{35}S]methionine-labeled viral particles in 0.4 ml regular medium were added to PT cells grown in 24-well plates. After 5 hr of incubation at 4°C, the cells were washed 3 times with ice-cold DMEM containing 1% FBS, scraped from the dish, and washed once more by centrifugation. Cells were collected in 100 μl medium, and the radioactivity was measured in 5 ml EcoLite+ scintillation fluid (ICI). For entry, both wt and mutant viruses (4 plus 4 wells of each, on separate 24-well plates) were adsorbed to the cells at 4°C for 5 hr. Later, the cells were washed twice with ice-cold DMEM containing 1% FBS before incubating 4 wells of each for 1, 3, 4 (at three different virus concentrations) and 5 hr at 37°C and 4 wells at 4°C, respectively. After the incubation, the cells were washed twice with DMEM containing 5 times-diluted porcine polyclonal anti-PPV antibody and 1% FBS and at last with DMEM containing 1% FBS at a pH of 8.5. The difference in cpm associated with the cells between the 37°C samples and 4°C (controls) after stripping with antibody accounted for the entry (error bars sum of those obtained at 4°C and 37°C). For entry into the nucleus 10^6 cpm [^{35}S]methionine-labeled viral particles in 5 ml regular medium were added to PT cells grown in 10 cm petri dishes. After 5 hr of incubation at at 4°C, the cells were washed once with regular medium and incubated at 37°C either for 1 or 16 hr. Cells were washed once with PBS and scraped from the dishes. Nuclear fraction purification was performed by a cellular fractionation method, based on plasma membrane lysis (Sperinde and Nugent, 1998). Less than 0.5% cytoplasmic contamination was found in the nuclear fraction in three separate fractionation procedures measuring the lactate dehydrogenase (LDH) activity by the Cytotoxicity Detection Kit (Roche Molecular Biochemicals). Integrity of the purified nuclei was confirmed by fluorescent microscopy after staining the nuclei with Hoechst 33258. Radioactivity of each cellular fraction was quantitated by counting in a liquid scintillation analyzer.

Acknowledgments

We thank Drs. S. Cotmore and P. Tattersall (Yale University), C. Parrish (Cornell University), M. Rossmann (Purdue University), and J.-F. Laliberté and F. Shareck (INRS-IAF) for suggestions and reading of the manuscript. P.T. is supported by the Natural Sciences and Engineering Research Council of Canada, Z.Z. at VMRI (Hungarian Academy of Sciences) by OTKA, and I.R.N. by the Canadian Institutes for Health Research.

Received December 26, 2000; revised July 13, 2001.

References

Balsinde, J., Balboa, M.A., Insel, P.A., and Dennis, E.A. (1999). Regulation and inhibition of phospholipase A2. Annu. Rev. Pharmacol. Toxicol. *39*, 175–189.

Bergeron, J., Menezes, J., and Tijssen, P. (1993). Genomic organization and mapping of transcription and translation products of the NADL-2 strain of porcine parvovirus. Virology *197*, 86–98.

Bergeron, J., Hebert, B., and Tijssen, P. (1996). Genome organization of the Kresse strain of porcine parvovirus: identification of the allotropic determinant and comparison with those of NADL-2 and field isolates. J. Virol. *70*, 2508–2515.

Berns, K.I. (1996). Parvoviridae: the viruses and their replication. In Fundamental Virology, Third Edition, B.N. Fields, D.M. Knipe, and P.M.Howley, eds. (Philadelphia, PA: Lippincott-Raven), pp. 1017–1041.

Brown, K.E. (2000). Haematological consequences of parvovirus B19 infection. Baillieres Best Pract. Res. Clin. Haematol. *13*, 245–259.

Brown, K.E., Anderson, S.M., and Young, N.S. (1993). Erythrocyte P antigen: cellular receptor for B19 parvovirus. Science *262*, 114–117.

Chapman, M.S., and Rossmann, M.G. (1993). Structure, sequence and function correlations among parvoviruses. Virology *194*, 491–508.

Cotmore, S.F., D'Abramo, M.A., Jr., Ticknor, C.M., and Tattersall, P. (1999). Controlled conformational transitions in the MVM virion expose the VP1 N-terminus and viral genome without particle disassembly. Virology *254*, 169–181.

Dennis, E.A. (1997). The growing phospholipase A2 superfamily of signal transduction enzymes. Trends Biochem. Sci. *22*, 1–2.

Dessen, A. (2000). Phospholipase A(2) enzymes: structural diversity in lipid messenger metabolism. Structure *8*, R15–R22.

Dijkstra, B.W., Drenth, J., and Kalk, K.H. (1981). Active site and catalytic mechanism of phospholipase A2. Nature *289*, 604–606.

Douar, A.M., Poulard, K., Stockholm, D., and Danos, O. (2001). Intracellular trafficking of adeno-associated virus vectors: routing to the late endosomal compartment and proteasome degradation. J. Virol. *75*, 1824–1833.

Duan, D., Li, Q., Kao, A.W., Yue, Y., Pessin, J.E., and Engelhardt, J.F. (1999). Dynamin is required for recombinant adeno-associated virus type 2 infection. J. Virol. *73*, 10371–10376.

Elsbach, P., and Weiss, J. (1991). Utilization of labeled Escherichia coli as phospholipase substrate. Methods Enzymol. *197*, 24–31.

Foto, F., Saag, K.G., Scharosch, L.L., Howard, E.J., and Naides, S.J. (1993). Parvovirus B19-specific DNA in bone marrow from B19 arthropathy patients: evidence for B19 virus persistence. J. Infect. Dis. *167*, 744–748.

Gardiner, E.M., and Tattersall, P. (1988). Evidence that developmentally regulated control of gene expression by a parvoviral allotropic determinant is particle mediated. J. Virol. *62*, 1713–1722.

Gelb, M.H., Cho, W., and Wilton, D.C. (1999). Interfacial binding of secreted phospholipase A_2: more than electrostatics and a major role for tryptophan. Curr. Opin. Struct. Biol. *9*, 428–432.

Geuze, H.J., Stoorvogel, W., Strous, G.J., Slot, J.W., Bleekemolen, J.E., and Mellman, I. (1988). Sorting of mannose-6-phosphate receptors and lysosomal membrane proteins in endocytic vesicles. J. Cell Biol. *107*, 2491–2501.

Griffiths, G., Hoflack, B., Simons, K., Mellman, I., and Kornfeld, S. (1988). The mannose-6-phosphate receptor and the biogenesis of lysosomes. Cell *52*, 329–341.

Haberhausen, G., Pinsl, J., Kuhn, C.C., and Markert-Hahn, C. (1998). Comparative study of different standardization concepts in quantitative competitive reverse transcription-PCR assays. J. Clin. Microbiol. *36*, 628–633.

Han, S.K., Kim, K.P., Koduri, R., Bittova, I., Munoz, N.M., Leff, A.R., Wilton, D.C., Gelb, M.H., and Cho, W. (1999). Role of Trp31 in high membrane binding and proinflammatory activity of human group V phospholipase A_2. J. Biol. Chem. *271*, 11881–11888.

Hansen, J., Qing, K., and Srivastava, A. (2001). Adeno-associated virus type 2-mediated gene transfer: altered endocytic processing enhances transduction efficiency in murine fibroblasts. J. Virol. *75*, 4080–4090.

Hariri, M., Millane, G., Guimond, M.-P., Guay, G., Dennis, J.W., and Nabi, I.R. (2000). Biogenesis of multilamellar bodies via autophagy. Mol. Biol. Cell *11*, 255–268.

Hermonat, P.L., Labow, M.A., Wright, R., Berns, K.I., and Muzyczka, N. (1984). Genetics of adeno-associated virus: isolation and preliminary characterization of adeno-associated virus type 2 mutants. J. Virol. *51*, 329–339.

Kasamatsu, H., and Nakanishi, A. (1998). How do animal DNA viruses get to the nucleus? Annu. Rev. Microbiol. *52*, 627–686.

Kramer, R.M., and Sharp, J.D. (1997). Structure, function and regulation of Ca^{2+}-sensitive cytosolic phospholipase A2 (cPLA2). FEBS Lett. *410*, 49–53.

Loizou, S., Cazabon, J.K., Walport, M.J., Tait, D., and So, A.K. (1997). Similarities of specificity and cofactor dependence in serum antiphospholipid antibodies from patients with human parvovirus B19 infection and from those with systemic lupus erythematosus. Arthritis Rheum. *40*, 103–108.

Manjunath, P., Soubeyrand, S., Chandonnet, L., and Roberts, K.D. (1994). Major proteins of bovine seminal plasma inhibit phospholipase A2. Biochem. J. *303*, 121–128.

Moore, T.L. (2000). Parvovirus-associated arthritis. Curr. Opin. Rheumatol. *12*, 289–294.

Murakami, M., Nakatani, Y., Atsumi, G., Inoue, K., and Kudo, I. (1997). Regulatory functions of phospholipase A_2. Crit. Rev. Immunol. *17*, 225–283.

Nabi, I.R., and Rodriguez-Boulan, E. (1993). Increased LAMP-2 polylactosamine glycosylation is associated with its slower Golgi transit during establishment of a polarized MDCK epithelial monolayer. Mol. Biol. Cell *4*, 627–635.

Nabi, I.R., Le Bivic, A., Fambrough, D., and Rodriguez-Boulan, E. (1991). An endogenous MDCK lysosomal membrane glycoprotein is targeted basolaterally before delivery to lysosomes. J. Cell Biol. *115*, 1573–1584.

Parker, J.S., and Parrish, C.R. (1997). Canine parvovirus host range is determined by the specific conformation of an additional region of the capsid. J. Virol. *71*, 9214–9222.

Parker, J.S., and Parrish, C.R. (2000). Cellular uptake and infection by canine parvovirus involves rapid dynamin-regulated chlatrin-mediated endocytosis, followed by slower intracellular trafficking. J. Virol. *74*, 1919–1930.

Parker, J.S., Murphy, W.J., Wang, D., O'Brien, S.J., and Parrish, C.R. (2001). Canine and feline parvoviruses can use human or feline transferrin receptors to bind, enter, and infect cells. J. Virol. *75*, 3896–3902.

Parrish, C.R. (1999). Host range relationships and the evolution of canine parvovirus. Vet. Microbiol. *69*, 29–40.

Previsani, N., Fontana, S., Hirt, B., and Beard, P. (1997). Growth of the parvovirus minute virus of mice MVMp3 in EL4 lymphocytes is restricted after cell entry and before viral DNA amplification: cell-specific differences in virus uncoating in vitro. J. Virol. *71*, 7769–7780.

Pruzanski, W., and Vadas, P. (1991). Phospholipase A2—a mediator between proximal and distal effectors of inflammation. Immunol. Today *12*, 143–146.

Qing, K., Mah, C., Hansen, J., Zhou, S., Dwarki, V., and Srivastava, A. (1999). Human fibroblast growth factor receptor 1 is a co-receptor for infection by adeno-associated virus 2. Nat. Med. *5*, 71–77.

Renetseder, R., Brunie, S., Dijkstra, B.W., Drenth, J., and Sigler, P.B. (1985). A comparison of the crystal structures of phospholipase A2 from bovine pancreas and Crotalus atrox venom. J. Biol. Chem. *260*, 11627–11634.

Rosenfeld, S.J., Yoshimoto, K., Kajigaya, S., Anderson, S., Young, N.S., Field, A., Warrener, P., Bansal, G., and Collett, M.S. (1992). Unique region of the minor capsid protein of human parvovirus B19 is exposed on the virion surface. J. Clin. Invest. *89*, 2023–2029. Erratum. J. Clin. Invest. *90*, 2609.

Sanlioglu, S., Benson, P.K., Yang, J., Atkinson, E.M., Reynolds, T., and Engelhardt, J.F. (2000). Endocytosis and nuclear trafficking of adeno-associated virus type 2 are controlled by rac1 and phosphatidylinositol-3 kinase activation. J. Virol. *74*, 9184–9196.

Sekar, K., and Sundaralingam, M. (1999). High-resolution refinement of orthorhombic bovine pancreatic phospholipase A2. Acta Crystallogr. D Biol. Crystallogr. *55*, 46–50.

Simpson, A.A., Chipman, P.R., Baker, T.S., Tijssen, P., and Rossmann, M.G. (1998). The structure of an insect parvovirus (Galleria mellonella densovirus) at 3.7 A resolution. Structure *6*, 1355–1367.

Sperinde, G.V., and Nugent, M.A. (1998). Heparan sulfate proteoglycans control intracellular processing of bFGF in vascular smooth muscle cells. Biochemistry. *37*, 13153–13164.

Summerford, C., Bartlett, J.S., and Samulski, R.J. (1999). αVβ5 integrin: a co-receptor for adeno-associated virus type 2 infection. Nat. Med. *5*, 78–82.

Takahashi, Y., Murai, C., Ishii, K., Sugamura, K., and Sasaki, T. (1998a). Human parvovirus B19 in rheumatoid arthritis. Int. Rev. Immunol. *17*, 309–321.

Takahashi, Y., Murai, C., Shibata, S., Munakata, Y., Ishii, K., Saitoh, T., Sawai, T., Sugamura, K., and Sasaki, T. (1998b). Human parvovirus B19 as a causative agent for rheumatoid arthritis. Proc. Natl. Acad. Sci. USA *95*, 8227–8232.

Tattersall, P., and Cotmore, S.F. (1990). Reproduction of autonomous parvovirus DNA. In Handbook of Parvoviruses, Vol. 1, P. Tijssen, ed. (Boca Raton, FL: CRC Press), pp. 123–140.

Tijssen, P., and Bergoin, M. (1995). Densonucleosis viruses constitute an increasingly diversified subfamily among the parvoviruses. Sem. Virol. *6*, 347–355.

Tullis, G.E., Burger, L.R., and Pintel, D.J. (1993). The minor capsid protein VP1 of the autonomous parvovirus minute virus of mice is dispensable for encapsidation of progeny single-stranded DNA but is required for infectivity. J. Virol. *67*, 131–141.

Vihinen-Ranta, M., Kalela, A., Makinen, P., Kakkola, L., Marjomaki, V., and Vuento, M. (1998). Intracellular route of canine parvovirus entry. J. Virol. *72*, 802–806.

Vihinen-Ranta, M., Yuan, W., and Parrish, C.R. (2000). Cytoplasmic trafficking of canine parvovirus capsid and its role in infection and nuclear transport. J. Virol. *74*, 4853–4859.

Weiner, M.P., Costa, G.L., Schoettlin, W., Cline, J., Mathur, E., and Bauer, J.C. (1994). Site-directed mutagenesis of double-stranded DNA by the polymerase chain reaction. Gene *151*, 119–123.

Willwand, K., and Kaaden, O.R. (1988). Capsid protein (p85) of Aleutian disease virus is a major DNA-binding protein. Virology *166*, 52–57.

Ytterberg, S.R. (1999). Viral arthritis. Curr. Opin. Rheumatol. *11*, 275–280.

Zhu, H., Dupureur, C.M., Zhang, X., and Tsai, M.D. (1995). Phospholipase A2 engineering. The roles of disulfide bonds in structure, conformational stability, and catalytic function. Biochemistry *34*, 15307–15314.